Archives of Phytopathology and Plant Protection

ISSN: 0323-5408 (Print) 1477-2906 (Online) Journal homepage: http://www.tandfonline.com/loi/gapp20

An artificial neural network approach to identify fungal diseases of cucumber (Cucumis sativus L.) plants using digital image processing

Keyvan Asefpour Vakilian & Jafar Massah

To cite this article: Keyvan Asefpour Vakilian & Jafar Massah (2013) An artificial neural network approach to identify fungal diseases of cucumber (Cucumis sativus L.) plants using digital image processing, Archives of Phytopathology and Plant Protection, 46:13, 1580-1588, DOI: 10.1080/03235408.2013.772321

To link to this article: https://doi.org/10.1080/03235408.2013.772321

Archives of Phytopathology and Plant Protection, 2013
Vol. 46, No. 13, 1580–1588, http://dx.doi.org/10.1080/03235408.2013.772321

An artificial neural network approach to identify fungal diseases of cucumber (*Cucumis sativus* L.) plants using digital image processing

Keyvan Asefpour Vakilian* and Jafar Massah

Department of Agrotechnology, University of Tehran, Tehran, Iran

(*Received 15 January 2013; final version received 29 January 2013*)

Nowadays, artificial intelligence solutions such as digital image processing and artificial neural networks (ANN) have become important applicable techniques in phytomonitoring and plant health detection systems. In this research, an autonomous device was designed and developed for detecting two types of fungi (*Pseudoperonospora cubensis*, *Sphaerotheca fuliginea*) that infect the cucumber (*Cucumis sativus* L.) plant leaves. This device was able to recognise the fungal diseases of plants by detecting their symptoms on plant leaves (downy mildew and powdery mildew). For leaves of cucumber inoculated with different spores of the fungi, it was possible to estimate the amount of hour post inoculation (HPI) by extracting leaves' image parameters. Device included a dark chamber, a CCD digital camera, a thermal camera, a light dependent resistor lightening module and a personal computer. The proposed programme for precise disease detection was based on an image processing algorithm and ANN. Three textural features and two thermal parameters from the obtained images were measured and normalised. Performance of ANN model was tested successfully for disease recognition and detecting HPI in images using back-propagation supervised learning method and inspection data. Such this machine vision system can be used in robotic intelligent systems to achieve a modern farmer's assistant in agricultural crop fields.

Keywords: artificial neural networks; downy mildew; fungal infection; powdery mildew; textural features; thermal parameters

1. Introduction

In recent years, image processing and machine vision systems have become important techniques in micro-precision agriculture. In the real-time phytomonitoring applications, high-quality machine vision systems are developed for non-contact sensing agricultural products (Huang et al. 2010). For example, they can identify emerging stresses and guide sampling for identification of the related stressor (Ushada et al. 2007). In traditional quantifying methods for plants' disease severity, visual estimation with illustrated diagrammatic scales, such as the drawings of various foliar diseases, is usually used (James 1971). Disease severity has also been quantified with leaf area metres (Sutton 1985), sunlight reflecting percentage and infrared radiation (Nutter et al. 1993). More recently, digital image acquisition systems have been used to assess fungal infection of fruits (Corkidi et al. 2006), viral infection of leaves (Martin and Rybicki 1998) and insect feeding (Alchanatis et al. 2000; Chen and Williams 2006).

*Corresponding author. Email: keyvan.asefpour@ut.ac.ir

Huang et al. (2007) derived photochemical reflectance index from both *in situ* spectral reflectance measurement and airborne hyper-spectral image to evaluate the yellow rust infection status in wheat. Qin et al. (2009) used colour camera and hyper-spectral imaging system to differentiate common symptomatic citrus diseases by taking pictures of citrus' leaves and fruit under laboratory environment. Li et al. (2012) set up a ground based prototype of hyper-spectral sensing system which was designed to identify citrus greening infected trees. Asefpour Vakilian and Massah (2012a) designed an automatic robot with real-time image processing system to detect nitrogen deficiency in greenhouse cucumber crops. Image textural features were extracted for calculating three parameters: entropy, energy and homogeneity.

Some researches have been done to develop a method for leaf colour analysis using image processing packages (Schaberg et al. 2003). In their research, the percentage of green and red colours in leaves of sugar maple (*Acer saccharum*) was measured to indicate the plant nutrition and health. Their method was adapted to quantify different fungal foliar diseases that cause changes in leaves' colour.

James (1971) showed that there is a high correlation between the percentage of diseased tissue measured by Scion Image analysis and the number of leaf spots. His method was tested on a range of naturally occurring foliar diseases: anthracnose caused by *Colletotrichum dematium* on *Convallaria majalis*, scab caused by *Venturia inaequalis* on *Malus domestica*, powdery mildew caused by *Oidium* sp. On *Phlox paniculata* and rust caused by *Coleosporium asterum* on *Solidago canadensis*.

Wijekoon et al. (2008) presented a method to quantify percentage of diseased leaf area using the Scion image software package (Scion Corporation, Frederick, MD) for anthracnose of *Nicotiana benthamiana* caused by *C. destructivum*, anthracnose of *C. majalis* leaves caused by *C. dematium*, scab caused by *V. inaequalis* in *M. domestica* leaves, powdery mildew in *Panus paniculata* leaves caused by *Oidium* sp. and rust in *S. canadensis* leaves caused by *C. asterum*.

El-Helly et al. (2003) developed an integrated image processing system to automate the inspection of leaf batches to identify the disease type. They showed that the leaf spots can be considered as an indicator of crop diseases. Pokharkar and Thool (2012) used an image segmentation method with Gaussian filter and Sobel operator to extract infected parts of particular plant's images.

Modern artificial neural networks (ANN) are non-linear statistical data modelling tools. They are usually used to model complex relationships between inputs and outputs or to find patterns in data. ANNs have the largest body of applications in agricultural and biological engineering when compared with other soft computing techniques (Huang et al. 2010). ANN models have the privilege of learning and simulating elaborate applications. Various researches have demonstrated that ANN models give a more accurate estimation in comparison with traditional statistical models (Ushada et al. 2007; Asefpour Vakilian and Massah 2013).

There are four types of fungi that seriously infect the cucumber (*Cucumis sativus* L.) plant leaves in Iran (24–40° N, 44–64° E): *Pseudoperonospora cubensis* (causes downy mildew), *Sphaerotheca fuliginea* (causes powdery mildew), *Colletotrichum lagenarium* (causes anthracnose) and *Alternaria cucumerina* (causes leaf blight).

The objectives of the current study were (1) to develop a machine vision system for automated identifying two types of fungi (*P. cubensis* and *S. fuliginea*) that infected the leaves of cucumber plants by using image textural features and thermal parameters and

(2) to improve the ability of proposed system to predict the hours post inoculation (HPI) for an infected leaf by utilising an ANN model.

2. Materials and methods

2.1. Plant material

Seeds of cucumber (*C. sativus* L.), susceptible to *P. cubensis* and *S. fuliginea,* were germinated on moist paper at 25/20 °C (day/night) for three days. Germinated seeds were transplanted into plastic pots with a mixture of organic soil and sand and were grown in a greenhouse at 25/20 °C (day/night) with an RH of 70 ± 10% and a photoperiod of 16 h/day (400 μmol m^{-2} s^{-1}). Plants were watered daily with tap water and were used for the experiments when the first true leaf had fully developed.

2.2. Plant inoculation for downy mildew infection

Sporulation of the pathogen was induced by placing plants with the first symptoms of downy mildew in a dark and moist chamber at 20 °C and 100% RH for 18 h. Leaves bearing zoosporangia were used directly for inoculation. Inoculation was done by means of an airbrush system using a suspension of $2 \times 10^4 - 5 \times 10^5$ sporangia ml^{-1} (0.01% Tween 20) depending on the disease severity desired. About 10 ml of zoosporangia suspension of *P. cubensis* was sprayed onto the lower surface of the first true leaves of cucumber plants.

2.3. Plant inoculation for powdery mildew infection

When the first true leaf of each cucumber plant was unfolded, the plants were inoculated with a single monospore isolate of *S. fuliginea*. Inoculation was done using a suspension of $2 \times 10^4 - 5 \times 10^5$ sporangia ml^{-1} (0.01% Tween 20) depending on the disease severity desired. About 10 ml of zoosporangia suspension of *S. fuliginea* was sprayed onto the lower surface of the first true leaves of cucumber plants.

2.4. Fungal infection assessment of plant leaves

After inoculation, plants were placed into a moist chamber at 25 °C under natural light conditions for 6 h in order to provide optimum infection conditions. For control, non-inoculated plants of the same age were kept under the same conditions. Subsequently, inoculated and control plants were kept in the greenhouse at 25/20 °C, 70 ± 10% RH and a photoperiod of 16 h (400 μE m^{-2} s^{-1}). Plants inoculated with pathogens were assessed daily for disease development.

At the first visible symptom, disease severity was assessed by visual rating of the percentage of leaf area showing characteristic symptoms of diseases. The necrotic area such as the yellowish halo and the faded area surrounding the lesions were all included in the assessment of disease severity. From each treatment group (non-inoculated, inoculated with *P. cubensis* and inoculated with *S. fuliginea*), 10 leaves were selected randomly once a day (at 24-h intervals) and transferred to a chamber for image acquisition for 10 days after inoculation. Therefore, 300 leaves were totally transferred during the experiments.

2.5. Image acquisition system

The elements of image acquisition system included five major units: a quite dark chamber, a CCD digital camera (Canon, Powershot, G12, Japan) for taking reflectance images, an infrared scanning camera (Testo881, Testo, USA) with a thermal sensitivity of 0.05 °C for taking thermal images, a light dependent resistor (LDR) lightening module and a personal computer. A 200-LEDs LDR array with view angle of 70° was used above the cameras to increase the light uniformity for the region of interest. Distance between the cameras and the samples were set about 20 cm. In general, air temperature and RH in the chamber were set to 25 °C and at 80% RH. Two sequential images were taken with cameras from each leaf, and these reflectance and thermal images were transferred to the computer, and then, image averaging was used for analysis to reduce the effect of random electronic noise and to reduce disturbances by factors that would cause the samples to move.

From each retrieved reflectance image, the region of interest (the leaf) was extracted from its background through an image segmentation process called Canny edge detection (Canny 1986). The images were converted to grey-scale image by forming a weighted sum of the R, G and B components. Figure 1 shows a reflectance image (Figure 1(a)) and a thermal image (Figure 1 (b)) for an inoculated cucumber plant leaf with *P. cubensis* and 96 h HPI. The programme for image processing system was written with MATLAB version 7.11 software (MATLAB 2010) using image processing toolbox.

2.6. Textural features extraction from the reflectance images

Gaunt (1987) presented a standard area diagram to score pathogen presence on a different scales of leaf area covered with symptoms visually. In this study, we did not use morphological features for image analysis because of their dependence to the distance between CCD camera and the leaves, and results may be varied in different experiments. The dimension of captured reflectance image was 1600×1200 pixels and was analysed as a raw bitmap image. Grey-level co-occurrence matrix was used to capture the spatial dependence of grey-level values for different angles of pixel relativity (0°,

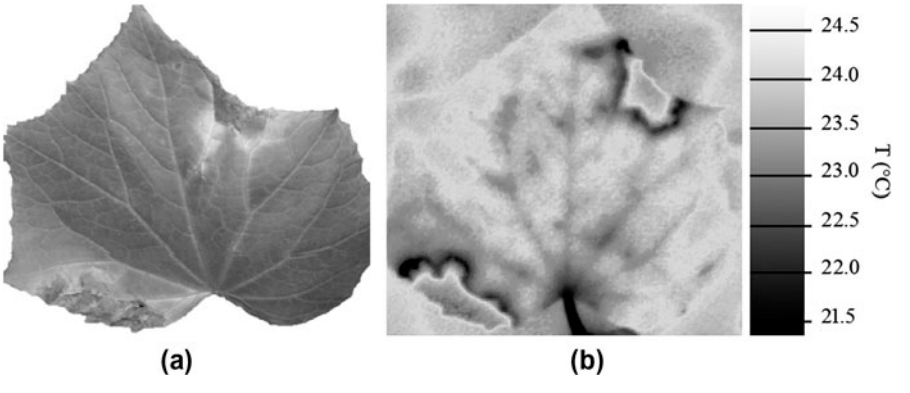

Figure 1. Images of a 96 HPI cucumber (*C. sativus* L.) leaf that affected with *P. cubensis* (a) reflectance image (b) thermal image. Regions of different temperature of cucumber leave are distinct in thermal image.

45°, 90° and 135°) (Jain et al. 1995). Each matrix was run through probability-density functions to calculate different textural parameters.

In one review, 21 textural parameters were identified (Zheng et al. 2006). However, another report indicated that only three textural parameters were useful in identifying plant health – entropy, energy and local homogeneity (Ushada et al. 2007; Story et al. 2010; Asefpour Vakilian and Massah 2012b). In this research, three textural parameters were extracted in identifying the disease type – entropy, energy and local homogeneity.

2.7. *Thermal features extraction from the thermal images*

Thermographic measurements such as leaf average temperature and maximum temperature difference (MTD) were calculated for every leaf that transferred to the chamber. MTD was automatically recorded as the difference between the highest and the lowest temperature within the region of interest (leaves).

2.8. *ANN model*

From 300 data sets obtained from images of healthy and infected plants, 250 data sets were used for training ANN model, while the remains were used as inspection data. The network was trained with Levenberg–Marquardt back-propagation algorithm. Therefore, the ANN architecture was considered as a 5–20–2 network which represents five nodes in the input layer, 20 nodes in the hidden layer and two nodes in the output layer was used for data analysis (Figure 2). Data sets of 20 leaf images were used for cross–validation, and remained 30 data sets were used for evaluating the presented ANN model in disease identification.

3. Results and discussion

Table 1 indicates an example of the training data. In order to choose the parameters (weights), the network was trained by training set. The process of cross-validation is used to monitor capability of the neural network to build generalised outputs. Lastly, testing data were used to validate the quality of proposed ANN model. Stop criteria and weight reset were used in order to cope with under fitting/over-fitting problems.

Comparison of training and inspection data were made in Figure 3 to show the closeness between the predicted and the measured value. The three axes represent training, validation and testing data. The dashed line in each axis represents the perfect

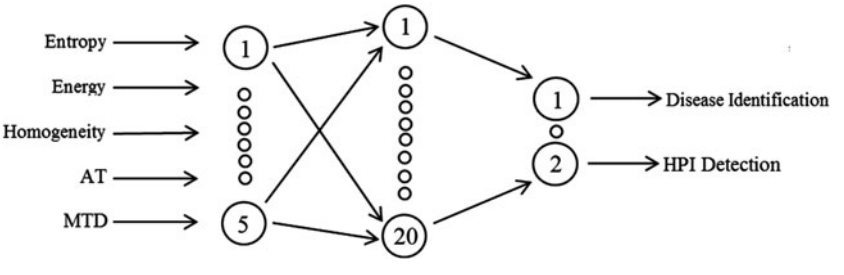

Figure 2. ANN architecture.

Table 1. Examples of the training data set.

Inputs					Output	
Entropy (pixels)	Energy (pixels)	Homogeneity (pixels)	AT (°C)	MTD (°C)	Disease identification	HPI detection
456,740	357,920	544,570	22.4	0.85	Non-inoculated	–
434,315	349,805	595,645	22.10	0.75	Non-inoculated	–
436,560	366,540	613,065	21.30	1.10	Downy mildew*	24
487,655	323,965	628,530	20.65	2.15	Downy mildew*	48
521,550	267,540	749,490	19.95	3.20	Downy mildew*	96
558,450	285,155	710,325	20.00	3.15	Downy mildew*	96
582,230	254,450	802,215	19.25	4.25	Downy mildew*	168
645,125	223,970	843,460	19.35	4.60	Downy mildew*	216
688,750	212,320	821,225	19.10	4.55	Downy mildew*	240
413,440	318,515	643,275	21.20	1.00	Powdery mildew**	36
429,905	327,050	658,710	21.05	1.15	Powdery mildew**	36
553,445	267,325	759,145	19.55	3.60	Powdery mildew**	120
551,230	213,230	798,310	19.80	3.95	Powdery mildew**	144
606,545	223,450	807,215	19.65	4.05	Powdery mildew**	168
612,230	243,460	803,460	19.30	4.45	Powdery mildew**	168
670,110	192,455	841,225	19.05	4.35	Powdery mildew**	240

*Inoculated with *P. cubensis*.
**Inoculated with *S. fuliginea*.

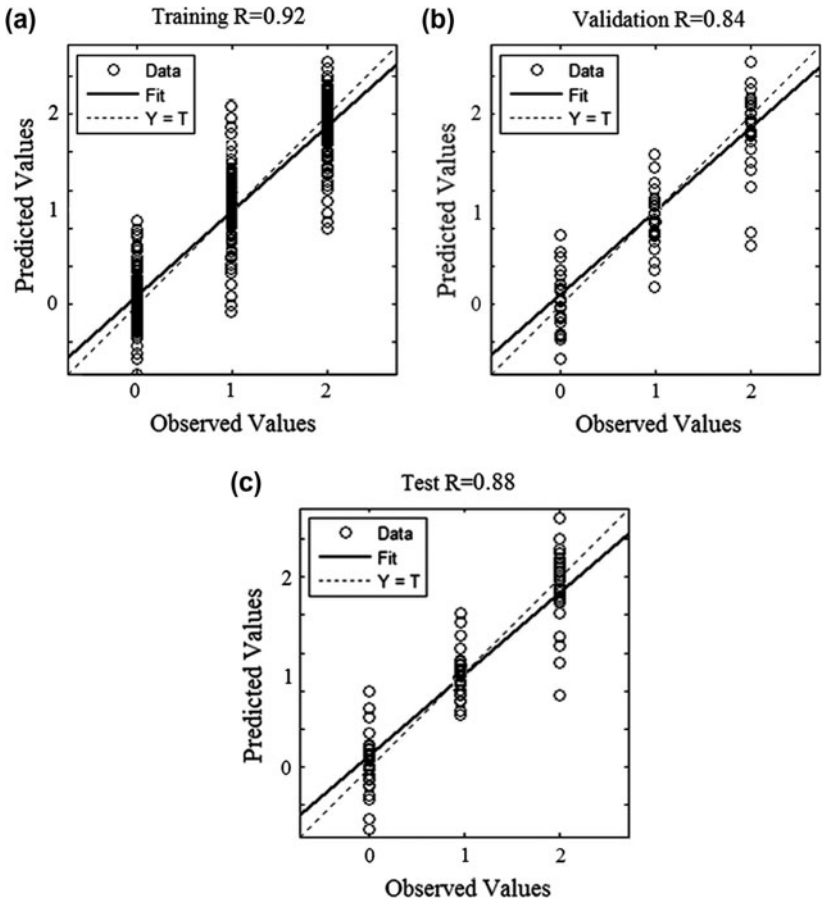

Figure 3. Regression results for proposed ANN model (a) training, (b) validation and (c) testing data. 0, 1 and 2 values in horizontal and vertical coordinates represent "non-inoculated", "inoculated with *P. cubensis*" and "inoculated with *S. fuliginea*", respectively.

result – predicted values = observed values. The solid line represents the best fit linear regression line between outputs and inputs. The *R* value is an indication of the relationship between the outputs and the inputs. In this study, the training data indicated a good fit.

The validation and test results also showed that the *R* values are about 0.9. In the best situation, this training stopped when the validation error increased for six iterations, which occurred at iteration 10.

In the textural analysis, entropy is defined as the randomness of grey-level distribution. As it is seen from input data sets of ANN model, the entropy value decreased due to a reduction in surface structure complexity during the time for inoculated plants' images. Energy is the numerical value represented by the level of grey-scale brightness. As the healthy plants became darker green in colour, the energy value decreased over time. Similarly, as the inoculated plants started to exhibit signs of fungal diseases, the yellowish appearance in the leaves resulted in a lighter colour and raised the energy levels in the images of the infected plants. Homogeneity is the determination of the related

grey-level pixel distribution amongst the surrounding pixels in the grey-scale image. As the control became colourful, with different shades of green, the related grey-level pixel distribution decreased over time. Conversely, the inoculated plants, being more unified in colour due to diseases, had higher grey-level pixel distribution values. These results confirm previous works studying on the effects of time on the values of textural features (Ushada et al. 2007; Story et al. 2010; Asefpour Vakilian and Massah 2012b).

The effects of *P. cubensis* infection on leaf temperature representing leaf transpiration during pathogenesis – decreasing the temperature due to the formation of chloroses – could also be demonstrated in the spatial distribution of leaf transpiration around infection sites (Oerke et al. 2006).

It seems that there were some statistical relations amongst estimating the proper value of HPI and textural and thermal parameters of the leaves' images. Although for detecting the disease type, ANN was used to increase the accuracy of disease identification.

4. Conclusion

In this study, a machine vision system was developed for a disease identification device. To improve the ability of the proposed system for identifying *P. cubensis* and *S. fuliginea* from each other on inoculated leaves' images, a back-propagation ANN model with three layers was utilised, and results showed that the ability of this system was acceptable. In commercial settings, it is desirable to develop an intelligent platform for real-time diseases identification. This could be achieved by a multi-sensing systems equipped with an artificial light source and a multi-sensor platform that moves in the crop fields and detects fungal diseases on plants' leaves. In order to increase the ability of intelligent farmer assistant robots in real-time detection of wide range of fungal and viral diseases, further researches need to be done by phytopathologists and agrotechnology engineers.

References

Alchanatis V, Navon A, Glazer L, Levski S. 2000. An image analysis system for measuring insect feeding effects caused by biopesticides. J Agric Eng Res. 77:289–296.

Asefpour Vakilian K, Massah J. 2012a. Design, development and performance evaluation of a robot to early detection of nitrogen deficiency in greenhouse cucumber (*Cucumis sativus*) with machine vision. Int J Agric Res Rev. 2(4):448–454.

Asefpour Vakilian K, Massah J. 2012b. Performance evaluation of CCD and CMOS cameras in image textural features extraction. Acta Technica Corviniensis. 5(3):61–64.

Asefpour Vakilian K, Massah J. 2013. Performance evaluation of a machine vision system for insect pests identification of field crops using artificial neural networks. Arch Phytopathol Plant Prot. http://dx.doi.org/10.1080/03235408.2013.763620

Canny J. 1986. A computational approach to edge detection. IEEE Trans Pattern Anal Mach Intell. 8(6):679–698.

Chen Y, Williams KA. 2006. Quantifying western flower thrips (*Frankliniella occidentalis* Pergande) (Thysanoptera: Thripidae) damage on ivy geranium (*Pelargonium peltatum* (L.) L'Her ex Ait.) (Geraniaceae Juss.) with adobe photoshop and scion image software. J Kansas Entomol Soc. 79:83–87.

Corkidi G, Balderas-Ruiz KA, Taboada B, Serrano-Carreon L, Galindo E. 2006. Assessing mango anthracnose using a new three-dimensional image-analysis technique to quantify lesions on fruit. Plant Pathol. 55:250–257.

El-Helly M, Rafea A, El-Gammal S. 2003. An integrated image processing system for leaf disease detection and diagnosis. Paper presented at: ICAIA 2003. Proceedings of 1st Indian International Conference on Artificial Intelligence; December 18–20; Hyderabad, India.

Gaunt RE. 1987. Crop loss assessment and pest management. St. Paul, MN: APS Press. Chapter 1, Measurement of disease and pathogens; p. 6–18.
Huang W, Lamb DW, Niu Z, Zhang Y, Liu L, Wang J. 2007. Identification of yellow rust in wheat using in-situ spectral reflectance measurements and airborne hyperspectral imaging. Precision Agric. 8(4–5):187–197.
Huang Y, Lan Y, Thomson SJ, Fang A, Hoffmann WC, Lacey RE. 2010. Development of soft computing and applications in agricultural and biological engineering. Comput Electron Agric. 71:107–127.
Jain R, Kasturi R, Schunck BG. 1995. Machine vision, 1st ed. New York (NY): McGraw-Hill.
James WC. 1971. An illustrated series of assessment keys for plant diseases, their preparation and usage. Can Plant Dis Surv. 51:39–65.
Li X, Lee WS, Li M, Ehsani R, Mishra AR, Yang C, Mangan RL. 2012. Spectral difference analysis and airborne imaging classification for citrus greening infected trees. Comput Electron Agric. 83:32–46.
Martin DP, Rybicki EP. 1998. Microcomputer-based quantification of maize streak virus symptoms in *Zea mays*. Phytopathology. 88:422–427.
MATLAB. 2010. MATLAB user's guide, version 7.11. Mathworks Ltd. USA.
Nutter FW, Jr, Gleason ML, Jenco JH, Christians NC. 1993. Assessing the accuracy, intra-rater repeatability and inter-rater reliability of disease assessment systems. Phytopathology. 83:806–812.
Oerke EC, Steiner U, Dehne HW, Lindenthal M. 2006. Thermal imaging of cucumber leaves affected by downy mildew and environmental conditions. J Exp Bot. 57(9):2121–2132.
Pokharkar SR, Thool VR. 2012. Early pest identification in greenhouse crops using image processing techniques. Int J Comput Sci Net. 1(3):162–167.
Qin J, Burks TF, Ritenour MA, Bonn WG. 2009. Detection of citrus canker using hyperspectral reflectance imaging with spectral information divergence. J Food Eng. 93(2):183–191.
Schaberg PG, Van Den Berg AK, Murakami PF, Shane JB, Donnelly JR. 2003. Factors influencing red expression in autumn foliage of sugar maple trees. Tree Physiol. 23:325–333.
Story D, Kacira M, Kubota C, Akoglu A, An L. 2010. Lettuce calcium deficiency detection with machine vision computed plant features in controlled environments. Comput Electron Agric. 74:238–243.
Sutton JC. 1985. Effectiveness of fungicides for managing foliar diseases and promoting yields of Ontario winter wheat. Phytoprotection. 66:141–152.
Ushada D, Murase H, Fukuda H. 2007. Non-destructive sensing and its inverse model for canopy parameters using texture analysis and artificial neural network. Comput Electron Agric. 57:149–165.
Wijekoon CP, Goodwin PH, Hsiang T. 2008. Quantifying fungal infection of plant leaves by digital image analysis using Scion Image software. J Microbiol Methods. 74:94–101.
Zheng C, Sun DW, Zheng L. 2006. Recent applications of image texture for evaluation of food qualities – a review. Trends Food Sci Technol. 17:113–128.